

Sodium–calcium exchange mediated contraction in left anterior descending and left ventricular branch arteries

Fareeha Qayyum^a, Imtisal Al-Bondokji^a, Iwona Kuszczak^b, Sue E. Samson^a, Ashok K. Grover^{a, b, *}

^a Department of Medicine, McMaster University, Hamilton, ON, Canada

^b Department of Biology, McMaster University, Hamilton, ON, Canada

Received: June 21, 2009; Accepted: July 27, 2009

Abstract

We tested the hypothesis that the de-endothelialized artery rings from the left anterior descending (LAD) coronary artery and its left ventricular branch (LVB) differ in their contractile responses to Na⁺–Ca²⁺-exchanger (NCX) mediated Ca²⁺-entry, muscarinic receptor activation with carbachol, and sarco/endoplasmic reticulum Ca²⁺ pump (SERCA) inhibition with thapsigargin. In LVB, the force of contraction (in N/g tissue) produced by the NCX mediated Ca²⁺-entry (17.5 ± 1.4) and carbachol (18 ± 1.5) was only slightly smaller than that due to membrane depolarization with KCl (24.0 ± 1.0). In contrast, in LAD the force of contraction produced with NCX (8.7 ± 0.7) and carbachol (6.1 ± 1.1) was much smaller than with KCl (15.7 ± 0.7). Thapsigargin also contracted LVB with greater force than LAD. When isolated microsomes were used, the binding to the muscarinic receptor antagonist quinuclidinyl benzilate was greater in LVB than in LAD. Microsomes were also used for Western blots. The intensities of signals for both SERCA and NCX were greater in LVB than in LAD. These biochemical observations were consistent with the contractile experiments. Thus, it appears that the differences between LAD and the resistance arteries may begin as early as LVB.

Keywords: NCX • NCX1 • SERCA2b • PMCA • muscarinic • conduit • resistance

Introduction

Coronary arteries supply the heart with blood containing oxygen and nutrients. Drastic changes in blood flow to the heart may lead to cardiac disorders [1–3]. The coronary tone is finely regulated by factors such as pH, pCO₂, membrane potential and by various hormones and neurotransmitters [4–13]. The epicardial and the left and right coronary arteries contribute 2–3% to coronary resistance, an additional contribution of 50% is due to branches with lumen diameters of 0.1 mm or more, and the remainder of the resistance is from small arterioles [14, 15]. However, this contribution may change with coronary spasm and with the site of myocardial infarction [15]. It is established that the regulatory properties of the conduit arteries differ from those of the arterioles but the regulation of the branch arteries and their role in controlling regional blood flow needs further investigation.

Branches from the left anterior descending (LAD) coronary artery include short branches that supply the septum or part of the

right ventricles and two to nine left ventricle branches (LVB) [16]. LVB supply the left ventricles which have a very high energy demand. In both diseased and healthy left ventricles, there is a regional non-uniformity of blood flow [17–20]. Acute occlusion of LVB is often used to examine local myocardial infarcts and various protective mechanisms including preconditioning [21, 22]. Small-vessel coronary artery disease can also cause classic angina pectoris [23]. In a study on human percutaneous coronary interventions for total occlusions, periprocedural myocardial infarction was attributed mainly to obstruction of side branches [24]. How this heterogeneity relates to characteristics and environments of the supplying blood vessels is not clear. There are only a limited number of pharmacological studies comparing LAD and the branch arteries. In organ bath studies, nitroglycerin relaxes dog large coronary artery rings (2 mm outer diameter) better than the smaller arteries (0.5 mm outer diameter) but relaxation with adenosine follows a reverse pattern [25]. In pig, as compared to the large coronary arteries, the subcellular fractions obtained from the small arteries are richer in adenosine receptors and 5'-nucleotidase and poorer in adenosine deaminase. Together, these differences may promote a prolonged action of adenosine in the smaller arteries [26]. The endothelium independent vasodilator calcitonin gene-related peptide is 10 times more potent in small

*Correspondence to: Dr. A.K. GROVER,
Department of Medicine, McMaster University,
Hamilton, Ontario L8N 3Z5, Canada.
Tel.: 905-525-9140 X22238
Fax: 905-522-3114
E-mail: groverak@mcmaster.ca

compared to large diameter artery rings. A repeated administration of this peptide to small artery rings does not cause tolerance, whereas in the large arteries a marked tolerance developed [27]. The large and small coronary arteries are also known to differ in their contraction *via* endothelin A and endothelin B receptors [28]. Since there is considerable heterogeneity in the blood supply to different parts of the heart and because left ventricles have the highest energy demand, the characteristics of LVB need close scrutiny.

The role of individual Ca^{2+} mobilization pathways in coronary artery contraction varies with each receptor. Actions of several agents affect cytosolic Ca^{2+} concentration ($[\text{Ca}^{2+}]_i$), which is key to cell signalling. $[\text{Ca}^{2+}]_i$ may be altered by Ca^{2+} entry into or exit from the cells or by Ca^{2+} release from or sequestration into internal sources. The pathways for increasing $[\text{Ca}^{2+}]_i$ include Ca^{2+} entry into the cells *via* voltage, receptor or store operated Ca^{2+} channels. The release of Ca^{2+} from the sarco/endoplasmic reticulum (SER) also increases $[\text{Ca}^{2+}]_i$. The mechanisms for lowering $[\text{Ca}^{2+}]_i$ include plasma membrane Ca^{2+} -pumps (PMCA) and SER Ca^{2+} -pumps (SERCA) [29–32]. Na^+ - Ca^{2+} -exchanger (NCX) plays a dual role. It exchanges three Na^+ for one Ca^{2+} and is non-rectorial; it may extrude Ca^{2+} from cells to decrease $[\text{Ca}^{2+}]_i$ or allow Ca^{2+} entry to increase $[\text{Ca}^{2+}]_i$ [33–36]. In fact, the Ca^{2+} entry *via* NCX may also contribute to Ca^{2+} refilling into the SER. NCXs are encoded by three genes: NCX1, 2 and 3. The NCX gene expressed in coronary artery smooth muscle is mainly NCX1. NCX1 may play a key role in contractility and this role may change with $[\text{Ca}^{2+}]_i$ overload and with lipid environment [37–41]. Here, we examine the role of NCX in the contractility of LVB and LAD. We determined the force of contraction produced by NCX mediated Ca^{2+} entry and by the activation of muscarinic receptors and compared it to the maximum force produced upon membrane depolarization. In order to interpret the differences in the force of contraction observed between the LAD and LVB, we also examined their morphology, muscarinic receptor binding and protein levels of NCX and SERCA2 in Western blots.

Methods

Contractility studies

Pig hearts were obtained from the slaughter house and placed immediately in chilled physiological saline solution (PSS, see Table 1 for buffer composition) until dissected. LAD and LVB were dissected from the hearts and placed in normal Krebs' solution bubbled with 95% O_2 and 5% CO_2 . The endothelium was removed as described previously [42]. Each artery was cut into 3-mm-long rings, which were mounted in an organ bath containing Krebs' solution at 37°C. Rings weighing 5–7 mg from the middle of LAD and those weighing 1.6–2 mg from LVB were used. In initial experiments, it was determined that the optimum tension was obtained with the LAD when they were placed under 3 g tension and after 30 min. The tension was readjusted back to 3 g. For LVB, the corresponding optimum value was 1.5 g. Each artery was contracted with 60 mM KCl, washed, con-

tracted again and the force of this second KCl contraction was recorded. The LADs were considered damaged and discarded if they generated less than $5 \times g$ force with KCl. The corresponding value for the LVB was 1 g. The tissues were then washed three times in Krebs' solution to relieve the tension caused by 60 mM KCl. In some tissues, responses to carbachol or thapsigargin in Krebs' solution were also examined.

To examine the effect of NCX mediated Ca^{2+} entry, the tissues were first Na^+ -loaded: placed in a K^+ - Ca^{2+} -free Krebs' solution for 20 min. and then in the Na^+ -loading solution for 60 min. [43]. The tissues were then washed and placed in Na^+ -containing (same as K^+ - Ca^{2+} -free) or in N-methylglucamine⁺ (NMG⁺)-containing (same as Na^+ -substituted) solutions. Immediately, CaCl_2 was added to obtain a final Ca^{2+} concentration of 1.5 mM or the concentration specified in other experiments. NCX mediated Ca^{2+} entry dependent contraction was determined as the difference between the contractions in the Na^+ -containing or the Na^+ -substituted solutions. In some experiments, the solutions also contained KB-R7943 (10 μM) or SEA 0400 (3 μM) resulting in 0.1% dimethylsulfoxide. Then the corresponding vehicle controls were also used.

Morphological studies

The de-endothelialized LAD and LVB were tested for contraction to 60 mM KCl as described above, washed, and then relaxed with 10 μM isoproterenol. LAD rings were mounted on stainless steel wire (2 mm thick) so as to prevent them from curving during the fixation step. A thinner wire (0.5 mm thick) was used for LVB. The wires with the mounted arteries were placed horizontally in formalin for 24–48 hrs. Further processing, embedding, sectioning and staining with haematoxylin and eosin were carried out at the Histology Facility in the Pathology department at McMaster University. The sections were examined for wall thickness using the software MultiGauge (Fujifilm Life Science, Stamford, CT, USA). Four photographs from different regions of each artery section were used for further analysis. In each photograph, the thickness of both the smooth muscle layer and the whole tissue were determined in six to eight places. More than 24 values of the smooth muscle layer thickness obtained from each tissue were summed up. Similarly, the thickness values for the whole tissues were also summed up. A ratio of the two summed thickness values was used to determine the smooth muscle to total tissue ratio for each ring.

Biochemical studies

The tissue was dissected and used for preparation of microsomes, as described previously [42, 44]. Briefly, the smooth muscle was dissected from pig LAD or LVB, and placed in ice-cold homogenization buffer (250 mM sucrose, 1 mM phenylmethylsulfonyl fluoride and 2 mM dithiothreitol). The tissue obtained with this procedure is predominantly smooth muscle – free of endothelium, adventitia, erythrocytes and cardiac myocytes. The tissues were homogenized and the microsomes were isolated by differential centrifugation [44]. The microsomes were suspended with 250 mM sucrose, stored frozen at -80°C , thawed within a few weeks and used for the appropriate experiments.

Specific binding to the muscarinic receptor antagonist ^3H -quinuclidinyl benzilate (QNB, PerkinElmer Canada, Woodbridge, Canada, 50.5 Ci/mmol) was determined in a buffer containing in mM: 100 NaCl, 10 MgCl_2 , 20 HEPES (4-(2-hydroxyethyl)-1-piperazineethane-sulfonic)-pH 7.5 [45, 46]. The microsomal membranes (40–100 μg protein) were mixed with QNB

Table 1 Composition of solutions used for contractility experiments

	PSS	Normal Krebs'	K ⁺ -Ca ²⁺ free Krebs'	Na ⁺ -loading solution	Na ⁺ -substituted solution
NaCl	134	115	120	120	
NaHCO ₃		22	22	22	22
NaH ₂ PO ₄			0.6	0.6	0.6
NMG ⁺ pH 7.4					120
KCl	6	5			
KH ₂ PO ₄		1.1			
MgCl ₂ /MgSO ₄	1	1.1	1.1	1.1	1.1
Glucose	10	7.77	7.77	7.77	7.77
CaCl ₂	2	2.2			
Ethylenediaminetetraacetic acid		0.03	0.03	0.03	0.03
Ethyleneglycol bis(b-aminoethyl ether)-N,N,N',N'-tetraacetic acid			0.1	0.1	0.1
HEPES-Na ⁺ , pH 6.4	10				
Nitrendipine			0.00005	0.00005	0.00005
Ouabain				0.1	
Nystatin				0.01	

All concentrations are in mM.

(0.2–2 nM) and incubated with 0 or excess atropine (20 μM, pA₂ = 9) for 90 min. at 22–24°C [46]. The membrane bound ligand was separated from the free ligand by vacuum filtration using 0.45 μm pore nitrocellulose filters, and the radioactivity level was determined by scintillation counting. The difference between the binding with and without atropine was taken as the specific binding.

Western blots were used to determine the relative abundance of SERCA2, NCX and PMCA proteins in microsomes isolated from the smooth muscle of LAD and LVB. The primary antibodies were purchased from the following sources: anti-SERCA2 antibody IID8 and anti-PMCA antibody 5F10 (Affinity Bioreagents, Golden, CO, USA) and anti-NCX1 antibody R3F1 (Swant Swiss Antibodies, Bellinzona, Switzerland). The Western blots were treated with the primary antibodies and then with the horseradish peroxidase conjugated antimouse IgG (GE Healthcare, Baie d'Urfe, Canada). The peroxidase activity was visualized with a femto-kit (Pierce Chemical Company, Rockford, IL, USA) and a LAS3000 mini Luminiscent Image Analyzer (Fujifilm Life Science). For each antibody, the relationship between the intensity and the protein amount was determined and only the protein amounts corresponding to the linear range were used for further analysis. For a given antibody on a single day, the mean of intensities/μg protein was determined for all samples of LAD. All the intensities/μg protein for LAD and LVB were computed relative to this mean value. The experiments were repeated on several days and the pooled values were used for computing the ratios shown in Table 2.

Data analysis

Values presented are mean ± S.E.M. of the specified number of replicates. Curve fitting was carried out using FigP software (Ancaster, Canada). Statistical significance was determined by one-way ANOVA and Tukey–Kramer multiple comparisons test using the software GraphPad Instat (SanDiego, CA, USA) or the Student's t-test when only two groups were compared. Values of $P < 0.05$ were considered to be significant.

Results

Characterization of NCX in LAD

Artery rings were Na⁺-loaded in organ baths and then placed in solutions containing Na⁺ or the Na⁺ substituent NMG⁺ (see Table 1 for compositions of the solutions). Then CaCl₂ was added to obtain a final Ca²⁺ concentration of 1.5 mM. The force of contraction was significantly greater for the tissues placed in the Na⁺-substituted solution than for those in the Na⁺ containing solution

Table 2 Comparison of main and branch arteries

	Main	Branch	Ratio (branch/main)
Force of contraction (N/g tissue weight)			
60 mM KCl	15.7 ± 0.7	24.1 ± 0.8	1.5 ± 0.1
NCX	8.7 ± 0.7	17.5 ± 1.4	2.0 ± 0.2
Carbachol	6.1 ± 1.2	18.0 ± 1.5	3.0 ± 0.2
Thapsigargin	0.4 ± 0.1	2.6 ± 0.5	6.5 ± 1.3
Relative smooth muscle content of artery wall			
Smooth muscle thickness/total artery wall thickness	0.49 ± 0.02	0.57 ± 0.03	1.2 ± 0.1
Muscarinic receptor binding (fmol/mg protein)			
QNB binding	38.9 ± 8.7	94.6 ± 18.9	2.4 ± 0.5
Western blots			
NCX1			3.2 ± 0.5
SERCA2			8.8 ± 1.8
PMCA			1.6 ± 0.2

Note: all values are mean ± S.E.M. Ratio values are (mean ± S.E.M. values for the branch artery)/(mean values for main artery). For Western blots, the number of comparisons for NCX1 = 7, for SERCA2 = 8 and 17 for PMCA.

(Fig. 1). The difference in the force of the contraction between the Na⁺-substituted and the Na⁺-containing solution was considered to be due to NCX-mediated Ca²⁺-entry. It is noted that the voltage dependent Ca²⁺ channels were blocked in these experiments with an excess of nitrendipine (50 nM, pA2 = 10) [47]. The NCX inhibitors KB-R7943 and SEA 0400 had no effect on the low level contraction in the Na⁺-containing solution (data not shown). In contrast, including them in the Na⁺-substituted solution resulted in significant decrease in the force of contraction (Fig. 1) [48–50]. In fact, the force of contraction in the presence of these two NCX inhibitors was comparable to that in the Na⁺-containing solution. These results thus validated this method for monitoring contraction due to the NCX mediated Ca²⁺ entry.

Contractile studies on LAD and LVB

The NCX mediated Ca²⁺ entry dependent contraction had similar EC50 values for extracellular Ca²⁺ for LAD (203 ± 43 μM) and LVB (231 ± 61 μM) (Fig. 2). The force of contraction due to muscarinic receptor activation in the two tissues was also compared at different concentrations of carbachol (Fig. 3). The EC50 values for carbachol were similar in LAD (0.46 ± 0.06 μM) and LVB (0.52 ± 0.18 μM) (Fig. 3).

Figure 4(A) compares the maximum force of contraction obtained in LAD rings with KCl (60 mM), NCX mediated Ca²⁺

entry (1.5 mM Ca²⁺), carbachol (3 μM) and the SERCA pump inhibitor thapsigargin (1 μM). The highest force of contraction was observed due to membrane depolarization with 60 mM KCl and the least with thapsigargin. The forces of contraction produced due to NCX mediated Ca²⁺ entry and carbachol were similar to each other and were 40–50% of the force with KCl. Figure 4(B) shows a similar comparison for LVB. Again, the highest force of contraction was observed with 60 mM KCl and the least with thapsigargin. The force of contractions produced by the NCX mediated Ca²⁺ entry and carbachol were similar to each other and were 70–75% of the force with KCl.

We also compared the contraction with each agent in LAD and LVB. With each agent, the force of contraction per mg tissue weight was significantly greater in LVB than in LAD. We also determined the ratios of these parameters in LVB to those in the LAD (Table 2). These ratios were thapsigargin (6.5 ± 1.3) > carbachol (3.0 ± 0.2) > NCX (2.0 ± 0.2) > KCl (1.5 ± 0.1). Thus, LAD and LVB differed in their contractions in a pathway dependent manner.

Smooth muscle content of LAD and LVB

The ratio of smooth muscle to total thickness in the arterial wall was determined as a measure of the relative proportion of smooth muscle content in each artery (Fig. 5). These values differed only

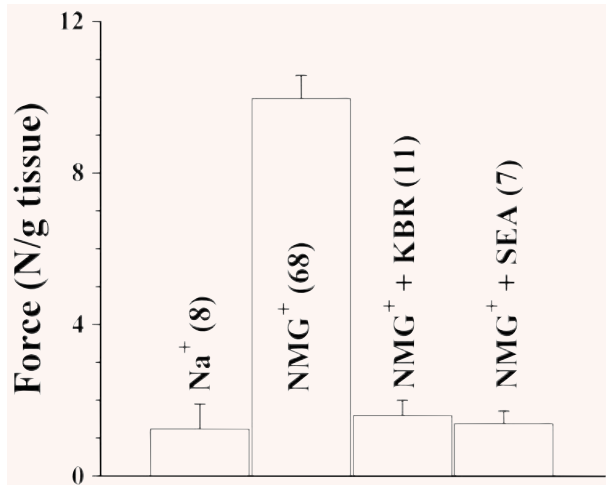


Fig. 1 Characterization of NCX in LAD. The Na⁺-loaded tissues were placed in Na⁺-containing or Na⁺-substituted solutions (NMG⁺). Where specified, the solutions also contained KB-R7943, (KBR) and SEA 0400 (SEA). The values given are mean \pm S.E.M. of the number of tissues indicated in parenthesis for each group. In the Tukey–Kramer multiple comparison test, $Q > 3.711$ signified that two groups differ from each other ($P < 0.05$). The analysis showed that the force of contraction in the tissues in NMG⁺ alone were significantly greater than in those with Na⁺ ($Q = 7.628$), NMG⁺ and KB-R7943 ($Q = 8.421$) or SEA 0400 ($Q = 7.067$). However, the groups Na⁺ versus NMG⁺ plus KB-R7943 ($Q = 0.246$), Na⁺ versus NMG⁺ plus SEA 0400 ($Q = 0.00834$) and NMG⁺ plus KB-R7943 versus NMG⁺ plus SEA 0400 ($Q = 0.1418$) did not differ significantly from each other.

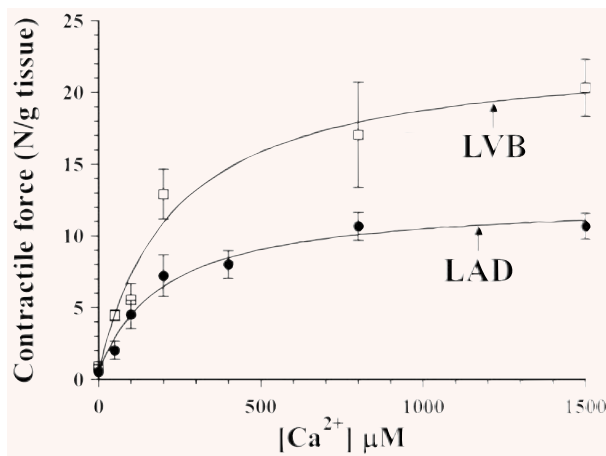


Fig. 2 Contraction due to NCX mediated Ca²⁺ entry in LAD and LVB. The Na⁺-loaded tissues were placed in Na⁺-substituted solutions (NMG⁺) and various concentrations of CaCl₂ to obtain the specified concentrations of Ca²⁺. The data fitted best with EC50 values of $203 \pm 43 \mu\text{M}$ ($r^2 = 0.9797$) and $231 \pm 61 \mu\text{M}$ ($r^2 = 0.9731$) for LAD and LVB, respectively.

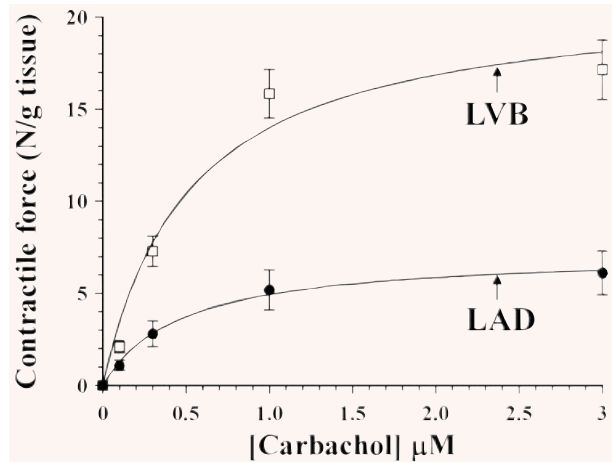


Fig. 3 Carbachol contraction in LAD and LVB. Graded dose responses were monitored in normal Krebs' solution containing 0, 0.1, 0.3, 1 and 3 μM carbachol. The data fitted best with EC50 values of $0.46 \pm 0.06 \mu\text{M}$ ($r^2 = 0.9756$) and $0.52 \pm 0.18 \mu\text{M}$ ($r^2 = 0.9957$) for LAD and LVB, respectively. The contraction per gram tissue was significantly greater in LVB than in LAD at all the concentrations of carbachol ($P < 0.05$).

marginally between the two arteries with the values in LAD (0.49 ± 0.02) being smaller than in LVB (0.57 ± 0.03).

Biochemical studies on microsomes from LAD and LVB

Specific binding to the muscarinic antagonist QNB was determined in microsomes prepared from LAD (Fig. 6A). The dissociation constant for the specific binding to QNB was $0.37 \pm 0.02 \text{ nM}$. Next, the specific binding at 2 nM QNB was compared in LAD and LVB (Fig. 6B). The specific binding was significantly greater in the microsomes from LVB than those from LAD.

Microsomes were used for Western blots to examine the relative abundance of NCX, SERCA2 and PMCA in LAD and LVB. To ensure that the differences observed in the Western blot were not artefacts of protein degradation, similar gels were used routinely stained with for proteins with Coomassie blue (data not shown). The signal intensity to protein plot for NCX was linear with LAD and LVB when up to 4 μg protein was used (Fig. 7). However, the slope of the graph was steeper with LVB than with LAD, indicating that NCX expression in LVB is greater than in LAD. For SERCA2, the signal intensity to protein plot with LAD was linear up to 4 μg protein but with LVB linearity was observed only when up to 2 μg protein was used (Fig. 8). The slope of the graph was steeper with LVB than with LAD, consistent with the SERCA2 expression being greater for LVB than for LAD. Figure 9 is a similar experiment showing linearity of signal for PMCA. The experiments in Figs 7, 8 and 9 are each from one gel and establish linearity of the range of protein amounts that could be used.

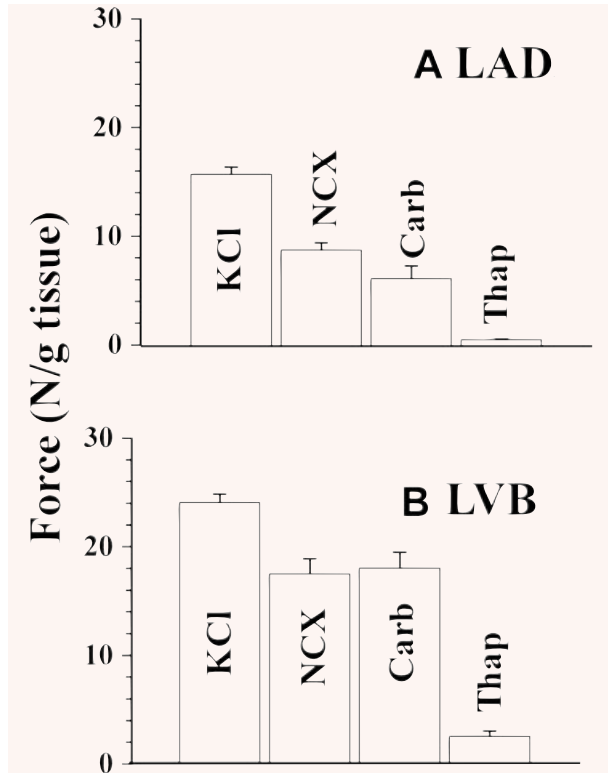


Fig. 4 Maximum force of contraction due to KCl, NCX, carbachol and thapsigargin. **(A)** LAD. The values are mean \pm S.E.M. of 80, 68, 12 and 12 tissues for KCl, NCX, carbachol and thapsigargin, respectively. Tukey–Kramer multiple comparison test showed that a Q -value $>$ 3.678 would signify that the two groups differed significantly from each other ($P <$ 0.05). The observed Q -values were KCl versus NCX: 11.161, KCl versus carbachol: 8.207, KCl versus thapsigargin: 13.063, NCX versus carbachol: 2.235, NCX versus thapsigargin: 7.036, carbachol versus thapsigargin: 3.682. **(B)** LVB. The values are mean \pm S.E.M. of 148, 39 and 36, and 12 tissues for KCl, NCX, carbachol and thapsigargin, respectively. Tukey–Kramer multiple comparison test showed that a Q -value $>$ 3.670 would signify that the two groups differed significantly from each other ($P <$ 0.05). The observed Q -values were KCl versus NCX: 5.671, KCl versus carbachol: 5.04, KCl versus thapsigargin: 11.153, NCX versus carbachol: 0.3637, NCX versus thapsigargin: 7.048, carbachol versus thapsigargin: 7.232.

Table 2 compares NCX, SERCA2 and PMCA in several such experiments using protein amounts only in the linear range. In each experiment the LVB/LAD intensity ratio was determined as described. The LVB/LAD ratios for this signal were SERCA2 $>$ NCX $>$ PMCA.

Discussion

LVB showed greater contraction due to the NCX-mediated Ca^{2+} -entry and carbachol stimulation than LAD. These results were con-

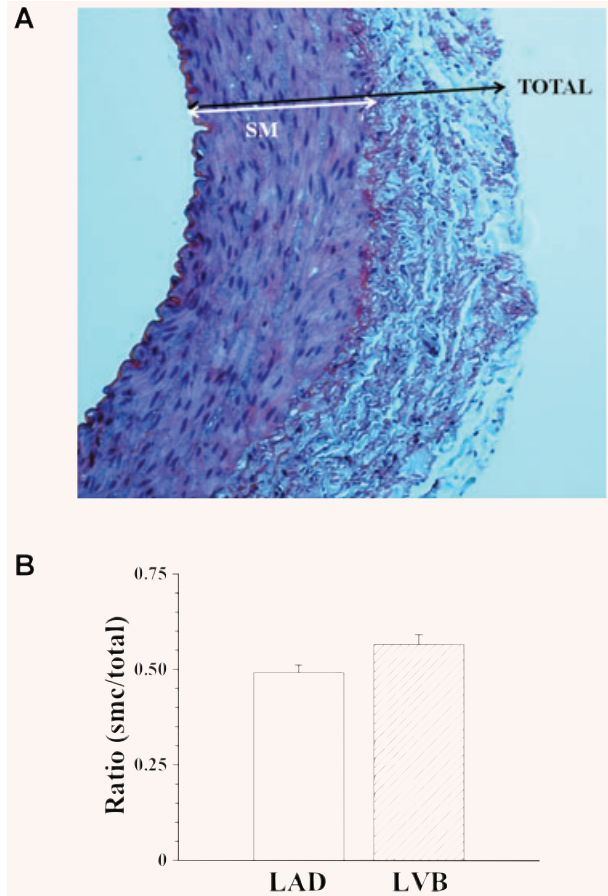


Fig. 5 Ratio of smooth muscle thickness to artery wall thickness of LAD and LVB. Mean \pm S.E.M. of seven values each. The values in the two groups differed significantly ($P = 0.041$).

sistent with greater abundance of the NCX protein and muscarinic receptors in LVB smooth muscle microsomes. Here, we focus on the validity of the methods used to obtain the results, comparison of the results with the literature on large and small arteries, and on possible implications of these observations.

We previously examined the NCX mediated Ca^{2+} -entry as radioactive Ca^{2+} uptake in cultured cells [43]. In that study, we Na^+ -loaded the cells and defined the NCX mediated Ca^{2+} -entry as the difference between the Ca^{2+} uptake in Na^+ -substituted and Na^+ -containing media. This uptake was inhibited by the reverse mode NCX inhibitors KB-R7943 (NCX) and SEA 0400 (NCX1) [48–50]. Therefore, we adopted this method to determine the contraction due to the NCX mediated Ca^{2+} -entry. We did observe a markedly larger contraction in the Na^+ -substituted than in the Na^+ -containing solutions. Then we verified that the contraction due to the NCX mediated Ca^{2+} -entry was inhibited by the NCX inhibitors KB-R7943 and SEA 0400. A caveat is that both the NCX inhibitors also block Ca^{2+} -entry via the L-type voltage operated Ca^{2+} channels [48]. However, here,

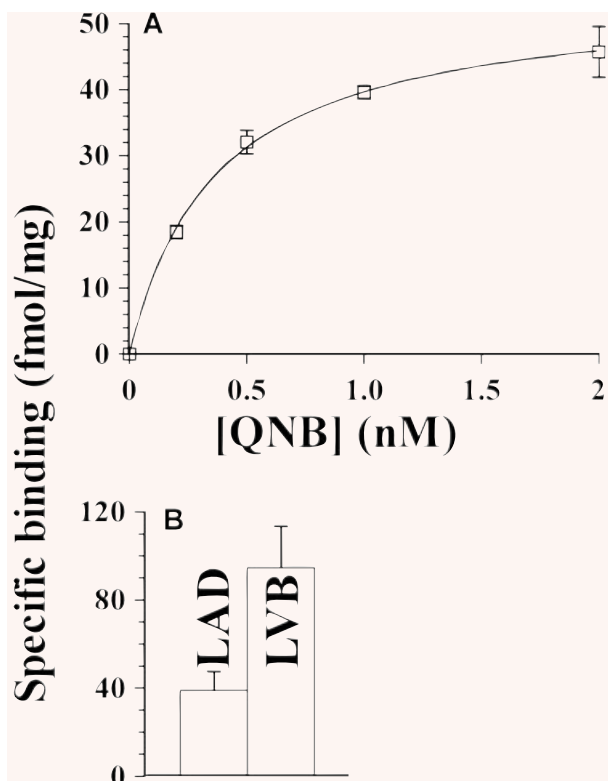


Fig. 6 Muscarinic receptor binding in LAD and LVB. **(A)** Concentration dependence of specific binding of QNB to the microsomes from LAD. The data fitted a single site binding curve with a K_D value of 0.37 ± 0.02 nM with $r^2 = 0.9992$. **(B)** Bar diagram comparing specific binding at 2 nM QNB in four experiments for LAD microsomes and three experiments for LVB. The binding was 39 ± 9 fmol/mg protein for the LAD microsomes and 95 ± 19 fmol/mg protein for LVB. The binding in the two groups differed significantly ($t = 2.952$, $df = 5$, $P = 0.038$).

this non-specific action of the NCX inhibitors is ruled out since the voltage dependent Ca^{2+} channels were already blocked with a high concentration of nitrendipine.

Table 2 summarizes the results on studies on contractility, morphology, receptor binding and Western blots. The larger contraction *via* the NCX-mediated Ca^{2+} entry in LVB is consistent with a greater abundance of NCX protein although differences in contractility regulation between the two arteries cannot be ruled out [48, 51, 52]. The larger contraction of LVB to carbachol correlates with the higher binding of QNB in LVB microsomes (Table 2). However, further differences may also exist between the muscarinic receptor pathways in the two arteries. Human coronary arteries express mRNA for both m2 and m3 receptors (and not m1 and m4), but it remains to be determined if LAD and LVB differ in relative abundance of the m2 and m3 receptor proteins, which act by different signal transduction pathways [53]. The greater abundance of the muscarinic receptors in LVB than in LAD is consistent with the observation that acetylcholine provokes more distal

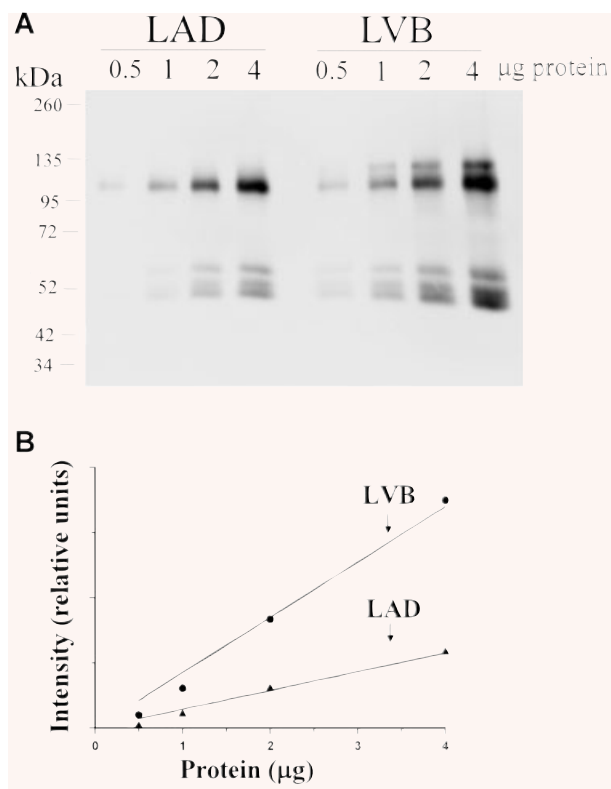


Fig. 7 Western blot analysis comparing NCX in LAD and LVB microsomes. **(A)** The amount of microsomal protein loaded from LAD and LVB is indicated for each lane. **(B)** The intensities of all the bands obtained in each lane were summed. The data for LAD fitted a straight line with an $r^2 = 0.9968$ and for LVB with $r^2 = 0.9990$.

spasms [54]. The larger contraction with thapsigargin also correlates with the greater abundance of the SERCA2 protein in LVB. Since the force of contraction per mg tissue was also slightly larger with KCl in LVB, we considered the possibility that there is a larger proportion of smooth muscle in LVB than in the LAD rings. However, a measurement of thickness of the smooth muscle layer to that of the total tissue showed only a marginal difference between the two arteries. Thus, additional factors may also contribute to the differences in the force of contraction.

NCX 1 and SERCA2 may contribute to the pathways involved in the activation of receptors. Hence, the observed differences between the LAD and LVB in NCX and SERCA2 suggest that the two arteries may differ in signalling steps that follow their receptor activation. Upon receptor activation, $[Ca^{2+}]_i$ may be increased by Ca^{2+} release from SER and this Ca^{2+} is then sequestered by SERCA2 into the SER. Thus, the greater abundance of SERCA2 in LVB may contribute to differences in the control of contractility in LVB and LAD. NCX has also been suggested to refill Ca^{2+} into the SER but refilling differences in LAD and LVB remain to be examined [55, 56]. The NCX1 knockout mice are embryolethal but the

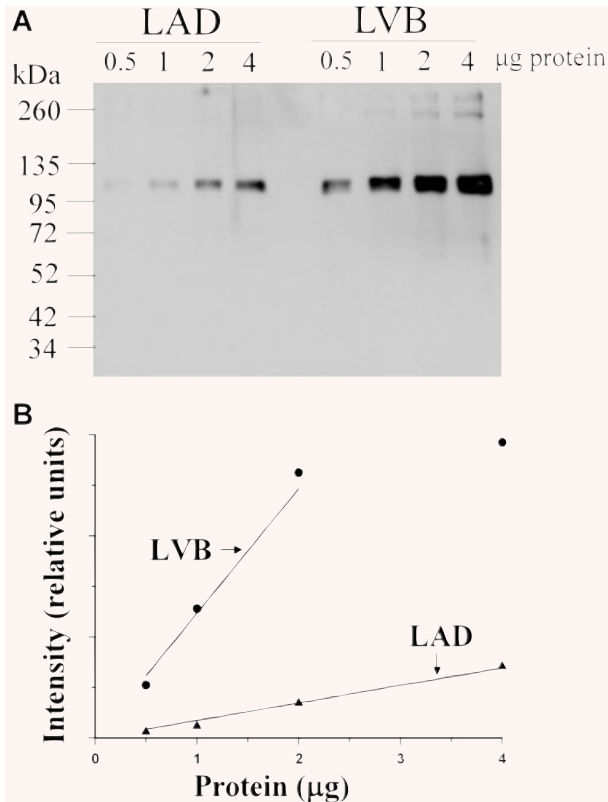


Fig. 8 Western blot analysis comparing SERCA2 in LAD and LVB microsomes. (A) The amount of microsomal protein loaded from LAD and LVB is indicated for each lane. (B) The intensities of all the bands obtained in each lane were summed. An intensity *versus* protein amount was linear for up to 2 μg protein for LVB. The data for LAD fitted a straight line with an $r^2 = 0.9969$. For LVB the data for up to 2 μg protein fitted with an $r^2 = 0.9991$.

knockout mice created by the Cre/loxP technology can adapt by altering expression of other Ca^{2+} transporters [38, 57, 58]. The depletion of NCX1 in postnatal rat myocytes using RNA interference results in a depressed $[Ca^{2+}]_i$ transient amplitude, a depressed rate of $[Ca^{2+}]_i$ rise and decline, elevated diastolic $[Ca^{2+}]_i$, and shorter action potentials, and a compensatory increase in PMCA expression. NCX1 gene splices encode several proteins of which NCX1.1 in the cardiac tissue and NCX1.3 in the coronary artery smooth muscle. The fatty acid α -linolenic acid inhibits both NCX1.1 and NCX1.3 but the latter is more sensitive to this inhibition [37]. NCX1.1 also differs from NCX1.3 in its response to $[Ca^{2+}]_i$ overload [39, 40].

Our observations add to the known differences between the LAD and smaller arteries. LAD and LVB differ in that the role of ETB receptors is greater in the latter. The large and small coronary arteries also differ in their response to angiotensin II, thapsigargin, peroxide, serotonin, nitroglycerin, $NaNO_2$, adenosine and α

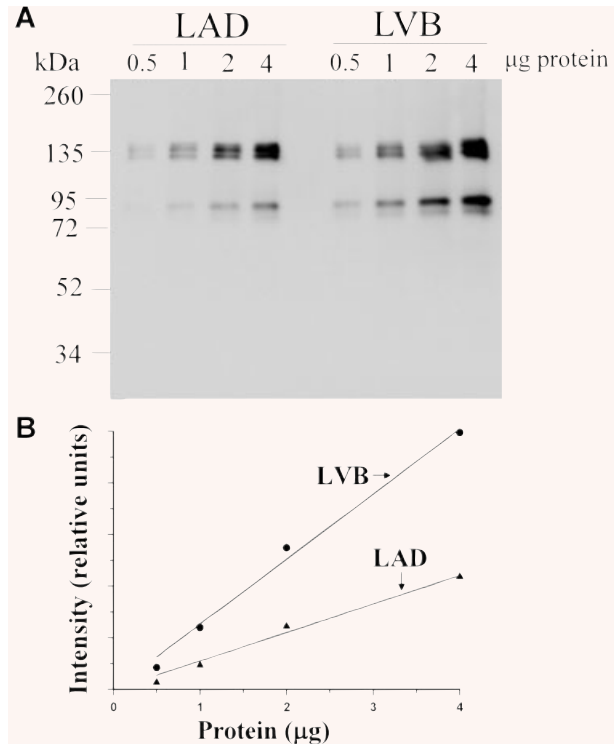


Fig. 9 Western blot analysis comparing PMCA in LAD and LVB microsomes. (A) The amount of microsomal protein loaded from LAD and LVB is indicated for each lane. (B) The intensities of all the bands obtained in each lane were summed. The data for LAD fitted a straight line with an $r^2 = 0.9978$ and for LVB with an $r^2 = 0.9925$.

adrenoceptor-mediated vasoconstriction [25, 59–62]. The smallest coronary arterioles have less eNOS protein per gram of total protein than the large coronary arteries [63]. Similar comparisons have also been made in other arteries. Nitric oxide and cGMP play a relatively greater role in the acetylcholine-induced dilatation of the aorta compared with the rat hindquarters resistance vasculature [11]. The angiotensin II-induced protein synthesis is associated with increased extracellular signal-regulated kinases 1/2 phosphorylation in aortic, but not in mesenteric vessels [64]. The differences between LAD and LVB may be attributed to their function. Even though they are both subsurface arteries, the primary role of LVB and its subendocardial branches is to supply the left ventricle which has a very high energy demand and produces a large force of contraction. The subendocardial flow is characterized by a noticeable systolic flow-velocity reversal which is contrasted to predominant forward-flow velocity during systole in the larger subsurface arteries [19, 20]. In dog, a dilated or failing left ventricle receives systolic flow to the outer myocardial layers, whereas at low preload levels myocardial perfusion occurs entirely during diastole [17]. These factors would suggest a different control of contractility in LVB than from LAD. Our observations on the

larger abundance of NCX, SERCA2 and muscarinic receptors in LVB are consistent with this assertion.

LAD and LVB may also respond differently to oxidative stress. LVB are rich in SERCA2 which is known to be readily damaged by peroxide, superoxide and peroxynitrite [65–67]. The endothelin response in LAD is mostly due to ETA receptors while in LVB it is due to both ETA and ETB; the ETB mediated contractions are sensitive to peroxide treatment [28, 68]. These differences in response to oxidative stress suggest that the functions of LAD and the LVB may also be altered differently in diabetes, atherosclerosis, and myocardial infarction [2, 3, 69, 70].

To summarize, LVB differs from LAD in the actions of nitroglycerine, adenosine, carbachol and endothelin receptor types, and in the relative abundance of the Ca^{2+} transporters SERCA2 and NCX.

Together, they point to a difference in the regulation of contractility in the two arteries, possibly a greater control of the tone of LVB than of LAD. These differences may be important for appropriate control of the blood supply to meet the high energy demand of the left ventricles.

Acknowledgements

We thank Drs. P.K. Rangachari and R.M.K.W. Lee for their suggestions, and Sara Praetorius, Sally Poon and Louise Murphy for assisting with some of the work. This work was supported by a Grant-in-Aid (T6168) from the Heart & Stroke Foundation of Ontario.

References

1. **Afzal N and Dhalla NS.** Sarcoplasmic reticular Ca^{2+} pump ATPase activity in congestive heart failure due to myocardial infarction. *Can J Cardiol.* 1996; 12: 1065–73.
2. **Duncker DJ, de Beer VJ, Merkus D.** Alterations in vasomotor control of coronary resistance vessels in remodelled myocardium of swine with a recent myocardial infarction. *Med Biol Eng Comput.* 2008; 46: 485–97.
3. **Range FT, Schafers M, Acil T et al.** Impaired myocardial perfusion and perfusion reserve associated with increased coronary resistance in persistent idiopathic atrial fibrillation. *Eur Heart J.* 2007; 28: 2223–30.
4. **Lui AH, McManus BM, Laher I.** Endothelial and myogenic regulation of coronary artery tone in the mouse. *Eur J Pharmacol.* 2000; 410: 25–31.
5. **Merkus D, Duncker DJ, Chilian WM.** Metabolic regulation of coronary vascular tone: role of endothelin-1. *Am J Physiol Heart Circ Physiol.* 2002; 283: H1915–21.
6. **Qin X, Zheng X, Qi H et al.** cGMP-dependent protein kinase in regulation of basal tone and in nitroglycerin- and nitric-oxide-induced relaxation in porcine coronary artery. *Pflugers Arch.* 2007; 454: 913–23.
7. **Rigel DF, Lappe RW.** Differential responsiveness of conduit and resistance coronary arteries to endothelin A and B receptor stimulation in anesthetized dogs. *J Cardiovasc Pharmacol.* 1993; 22: S243–7.
8. **Tousoulis D, Charakida M, Stefanadis C.** Endothelial function and inflammation in coronary artery disease. *Postgrad Med J.* 2008; 84: 368–71.
9. **Weirich J, Dumont L, Fleckenstein-Grun G.** Contribution of store-operated Ca^{2+} entry to pHo-dependent changes in vascular tone of porcine coronary smooth muscle. *Cell Calcium.* 2004; 35: 9–20.
10. **Weirich J, Dumont L, Fleckenstein-Grun G.** Contribution of capacitative and non-capacitative Ca^{2+} -entry to M3-receptor-mediated contraction of porcine coronary smooth muscle. *Cell Calcium.* 2005; 38: 457–67.
11. **Woodman OL, Wongsawatkul O, Sobey CG.** Contribution of nitric oxide, cyclic GMP and K^{+} channels to acetylcholine-induced dilatation of rat conduit and resistance arteries. *Clin Exp Pharmacol Physiol.* 2000; 27: 34–40.
12. **Xu XP, Liu Y, Tanner MA et al.** Differences in nitric oxide production in porcine resistance arteries and epicardial conduit coronary arteries. *J Cell Physiol.* 1996; 168: 539–48.
13. **Yamaguchi O, Kaneshiro T, Saitoh S et al.** Regulation of coronary vascular tone via redox modulation in the $\{\alpha\}$ 1-adrenergic-angiotensin-endothelin axis of the myocardium. *Am J Physiol Heart Circ Physiol.* 2009; 296: H226–32.
14. **Chilian WM, Eastham CL, Marcus ML.** Microvascular distribution of coronary vascular resistance in beating left ventricle. *Am J Physiol.* 1986; 251: H779–88.
15. **Vatner SF, Hintze TH.** Effects of a calcium-channel antagonist on large and small coronary arteries in conscious dogs. *Circulation.* 1982; 66: 579–88.
16. **Standring S.** Gray's anatomy, the anatomical basis of clinical practice. 39th ed. Edinburgh: Churchill Livingstone; 2005.
17. **Archie JP, Jr.** Intramyocardial pressure: effect of preload on transmural distribution of systolic coronary blood flow. *Am J Cardiol.* 1975; 35: 904–11.
18. **Bogaert J, Rademakers FE.** Regional nonuniformity of normal adult human left ventricle. *Am J Physiol Heart Circ Physiol.* 2001; 280: H610–20.
19. **Flynn AE, Coggins DL, Goto M et al.** Does systolic subepicardial perfusion come from retrograde subendocardial flow? *Am J Physiol.* 1992; 262: H1759–69.
20. **Toyota E, Ogasawara Y, Hiramatsu O et al.** Dynamics of flow velocities in endocardial and epicardial coronary arterioles. *Am J Physiol Heart Circ Physiol.* 2005; 288: H1598–603.
21. **McGuinness J, Neilan TG, Cummins R et al.** Intravenous glutamine enhances COX-2 activity giving cardioprotection. *J Surg Res.* 2008; 152: 140–7.
22. **Sakabe M, Shiroshita-Takeshita A, Maguy A et al.** Effects of a heat shock protein inducer on the atrial fibrillation substrate caused by acute atrial ischaemia. *Cardiovasc Res.* 2008; 78: 63–70.
23. **Mosseri M, Yarom R, Gotsman MS et al.** Histologic evidence for small-vessel coronary artery disease in patients with angina pectoris and patent large coronary arteries. *Circulation.* 1986; 74: 964–72.
24. **Paizis I, Manginas A, Voudris V et al.** Percutaneous coronary intervention for chronic total occlusions: the role of

- side-branch obstruction. *EuroIntervention*. 2009; 4: 600–6.
25. **Schnaar RL, Sparks HV.** Response of large and small coronary arteries to nitroglycerin, NaNO₂, and adenosine. *Am J Physiol*. 1972; 223: 223–8.
 26. **Grover AK, Samson SE, Lee RM.** Adenosine metabolism in small coronary arteries of pig. *Biochem Int*. 1992; 27: 717–24.
 27. **Foulkes R, Shaw N, Bose C et al.** Differential vasodilator profile of calcitonin gene-related peptide in porcine large and small diameter coronary artery rings. *Eur J Pharmacol*. 1991; 201: 143–9.
 28. **Elmoselhi AB, Grover AK.** ET(B)-mediated contraction differs between left descending coronary artery and its next branch. *Mol Cell Biochem*. 1999; 201: 99–103.
 29. **Carafoli E.** Calcium signaling: a tale for all seasons. *Proc Natl Acad Sci USA*. 2002; 99: 1115–22.
 30. **Misquitta CM, Mack DP, Grover AK.** Sarco/endoplasmic reticulum Ca²⁺ (SERCA)-pumps: link to heart beats and calcium waves. *Cell Calcium*. 1999; 25: 277–90.
 31. **Shull GE, Okunade G, Liu LH et al.** Physiological functions of plasma membrane and intracellular Ca²⁺ pumps revealed by analysis of null mutants. *Ann N Y Acad Sci*. 2003; 986: 453–60.
 32. **Strehler EE, Treiman M.** Calcium pumps of plasma membrane and cell interior. *Curr Mol Med*. 2004; 4: 323–35.
 33. **Blaustein MP, Lederer WJ.** Sodium/calcium exchange: its physiological implications. *Physiol Rev*. 1999; 79: 763–854.
 34. **Condrescu M, Opuni K, Hantash BM et al.** Cellular regulation of sodium-calcium exchange. *Ann N Y Acad Sci*. 2002; 976: 214–23.
 35. **Dong H, Dunn J, Lytton J.** Stoichiometry of the Cardiac Na⁺/Ca²⁺ exchanger NCX1.1 measured in transfected HEK cells. *Biophys J*. 2002; 82: 1943–52.
 36. **Philipson KD, Nicoli DA, Ottolia M et al.** The Na⁺/Ca²⁺ exchange molecule: an overview. *Ann N Y Acad Sci*. 2002; 976: 1–10.
 37. **Ander BP, Hurtado C, Raposo CS et al.** Differential sensitivities of the NCX1.1 and NCX1.3 isoforms of the Na⁺-Ca²⁺ exchanger to alpha-linolenic acid. *Cardiovasc Res*. 2007; 73: 395–403.
 38. **Henderson SA, Goldhaber JI, So JM et al.** Functional adult myocardium in the absence of Na⁺-Ca²⁺ exchange: cardiac-specific knockout of NCX1. *Circ Res*. 2004; 95: 604–11.
 39. **Hurtado C, Ander BP, Maddaford TG et al.** Adenovirally delivered shRNA strongly inhibits Na⁺-Ca²⁺ exchanger expression but does not prevent contraction of neonatal cardiomyocytes. *J Mol Cell Cardiol*. 2005; 38: 647–54.
 40. **Hurtado C, Prociuk M, Maddaford TG et al.** Cells expressing unique Na⁺/Ca²⁺ exchange (NCX1) splice variants exhibit different susceptibilities to Ca²⁺ overload. *Am J Physiol Heart Circ Physiol*. 2006; 290: H2155–62.
 41. **Szewczyk MM, Davis KA, Samson SE et al.** Ca²⁺-pumps and Na⁺-Ca²⁺-exchangers in coronary artery endothelium versus smooth muscle. *J Cell Mol Med*. 2007; 11: 129–38.
 42. **Grover AK, Samson SE.** Peroxide resistance of ER Ca²⁺ pump in endothelium: implications to coronary artery function. *Am J Physiol*. 1997; 273: C1250–8.
 43. **Davis KA, Samson SE, Hammel KE et al.** Functional linkage of Na(+)-Ca(2+)-exchanger to sarco/endoplasmic reticulum Ca(2+) pump in coronary artery: comparison of smooth muscle and endothelial cells. *J Cell Mol Med* "Postprint". Doi: 10.1111/j.1582-4934.2008.00480.x.
 44. **Grover AK, Samson SE, Lee RM.** Subcellular fractionation of pig coronary artery smooth muscle. *Biochim Biophys Acta*. 1985; 818: 191–9.
 45. **Entzeroth M, Doods HN, Mayer N.** Characterization of porcine coronary muscarinic receptors. *Naunyn Schmiedebergs Arch Pharmacol*. 1990; 341: 432–8.
 46. **Yamada S, Yamazawa T, Nakayama K.** Direct binding and functional studies on muscarinic cholinergic receptors in porcine coronary artery. *J Pharmacol Exp Ther*. 1990; 252: 765–9.
 47. **Grover AK, Oakes PJ.** Calcium channel antagonist binding and pharmacology in rat uterine smooth muscle. *Life Sci*. 1985; 37: 2187–92.
 48. **Birinyi P, Acsai K, Banyasz T et al.** Effects of SEA0400 and KB-R7943 on Na⁺/Ca²⁺ exchange current and L-type Ca²⁺ current in canine ventricular cardiomyocytes. *Naunyn Schmiedebergs Arch Pharmacol*. 2005; 372: 63–70.
 49. **Iwamoto T, Watano T, Shigekawa M.** A novel isothiourea derivative selectively inhibits the reverse mode of Na⁺/Ca²⁺ exchange in cells expressing NCX1. *J Biol Chem*. 1996; 271: 22391–7.
 50. **Iwamoto T.** Forefront of Na⁺/Ca²⁺ exchanger studies: molecular pharmacology of Na⁺/Ca²⁺ exchange inhibitors. *J Pharmacol Sci*. 2004; 96: 27–32.
 51. **Cheung JY, Rothblum LI, Moorman JR et al.** Regulation of cardiac Na⁺/Ca²⁺ exchanger by phospholemman. *Ann N Y Acad Sci*. 2007; 1099: 119–34.
 52. **Mizuno Y, Isotani E, Huang J et al.** Myosin light chain kinase activation and calcium sensitization in smooth muscle in vivo. *Am J Physiol Cell Physiol*. 2008; 295: C358–64.
 53. **Niihashi M, Esumi M, Kusumi Y et al.** Expression of muscarinic receptor genes in the human coronary artery. *Angiology*. 2000; 51: 295–300.
 54. **Sueda S, Kohno H, Fukuda H et al.** Induction of coronary artery spasm by two pharmacological agents: comparison between intracoronary injection of acetylcholine and ergonovine. *Coron Artery Dis*. 2003; 14: 451–7.
 55. **Lee CH, Poburko D, Kuo KH et al.** Relationship between the sarcoplasmic reticulum and the plasma membrane. *Novartis Found Symp*. 2002; 246: 26–41.
 56. **van Breemen C, Chen Q, Laher I.** Superficial buffer barrier function of smooth muscle sarcoplasmic reticulum. *Trends Pharmacol Sci*. 1995; 16: 98–105.
 57. **Cho CH, Kim SS, Jeong MJ et al.** The Na⁺-Ca²⁺ exchanger is essential for embryonic heart development in mice. *Mol Cells*. 2000; 10: 712–22.
 58. **Koushik SV, Wang J, Rogers R et al.** Targeted inactivation of the sodium-calcium exchanger (Ncx1) results in the lack of a heartbeat and abnormal myofibrillar organization. *FASEB J*. 2001; 15: 1209–11.
 59. **Grover AK, Samson SE, Misquitta CM et al.** Effects of peroxide on contractility of coronary artery rings of different sizes. *Mol Cell Biochem*. 1999; 194: 159–64.
 60. **Gutterman DD, Rusch NJ, Hermsmeyer K et al.** Differential reactivity to 5-hydroxytryptamine in canine coronary arteries. *Blood Vessels*. 1986; 23: 165–72.
 61. **Harder DR, Belardinelli L, Sperelakis N et al.** Differential effects of adenosine and nitroglycerin on the action potentials of large and small coronary arteries. *Circ Res*. 1979; 44: 176–82.
 62. **Misquitta CM, Samson SE, Grover AK.** Sarcoplasmic reticulum Ca(2+)-pump density is higher in distal than in proximal segments of porcine left coronary artery. *Mol Cell Biochem*. 1996; 158: 91–5.
 63. **Laughlin MH, Turk JR, Schrage WG et al.** Influence of coronary artery diameter on eNOS protein content. *Am J Physiol Heart Circ Physiol*. 2003; 284: H1307–12.

64. **Daigle C, Martens FM, Girardot D *et al.*** Signaling of angiotensin II-induced vascular protein synthesis in conduit and resistance arteries *in vivo*. *BMC Cardiovasc Disord.* 2004; 4: 6.
65. **Grover AK, Samson SE.** Effect of superoxide radical on Ca²⁺ pumps of coronary artery. *Am J Physiol.* 1988; 255: C297–303.
66. **Grover AK, Samson SE, Robinson S *et al.*** Effects of peroxynitrite on sarcoplasmic reticulum Ca²⁺ pump in pig coronary artery smooth muscle. *Am J Physiol Cell Physiol.* 2003; 284: C294–301.
67. **Grover AK, Samson SE, Fomin VP.** Peroxide inactivates calcium pumps in pig coronary artery. *Am J Physiol.* 1992; 263: H537–43.
68. **Elmoselhi AB, Grover AK.** Peroxide sensitivity of endothelin responses in coronary artery smooth muscle: ET(A) vs. ET(B) pathways. *Mol Cell Biochem.* 1999; 202: 47–52.
69. **Gurney AM, Howarth FC.** Effects of streptozotocin-induced diabetes on the pharmacology of rat conduit and resistance intrapulmonary arteries. *Cardiovasc Diabetol.* 2009. Doi: 10.1186/1475–2840-8–4.
70. **Liao JK, Bettmann MA, Sandor T *et al.*** Differential impairment of vasodilator responsiveness of peripheral resistance and conduit vessels in humans with atherosclerosis. *Circ Res.* 1991; 68: 1027–34.